

Annett Gebert,
 Nahla Ismail,
 Ulrike Wolff,
 Margitta Uhlemann,
 Frank Schneider,
 Jürgen Eckert
 and Ludwig Schultz

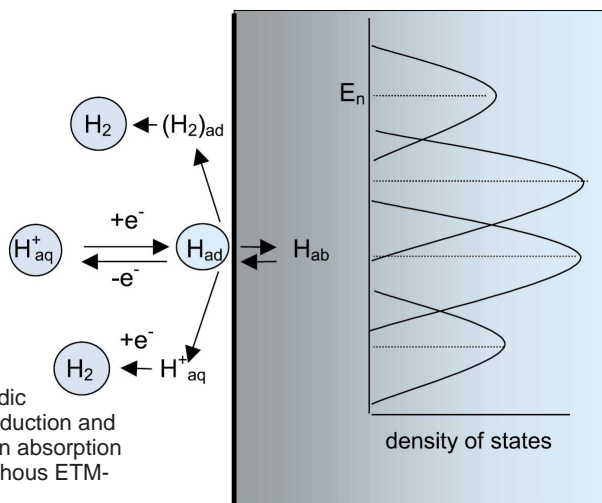
Electrochemical properties of bulk glass-forming Zr-based alloys

Recently developed bulk glass-forming alloy systems [1,2] have caught much attention not only due to their ease of preparation and their multicomponent glassy nature yielding new interest for basic research, but also due to expected novel properties and the prospec-

tive high potential for applications. Bulk amorphous Zr-based alloys exhibit interesting mechanical properties, i.e. extremely high yield strength combined with a relatively low Young's modulus at ambient temperatures as well as Newtonian flow in the supercooled liquid state [3]. However, applications of these materials require also high stability in various environments in order to ensure an acceptable lifetime. In general, the electrochemical reactivity of amorphous alloys in comparison to that of crystalline materials must be considered in terms of structure, chemical composition and homogeneity [4]. For bulk amorphous Zr-Al-Cu-Ni alloys an improved anodic passivation behaviour in various electrolytes at room temperature as compared to that of the multiphase crystalline alloy was detected. Under hot water conditions up to 250°C more porous and, thus, more permeable oxide layers form. In chloride solutions, bulk amorphous alloy samples are susceptible to pitting caused by the existence of microcrystalline inclusions formed during the preparation due to impurities in the melt [5]. These results show that further optimisation of alloy composition and microstructure is necessary to attain high corrosion resistance. This is subject of current investigations.

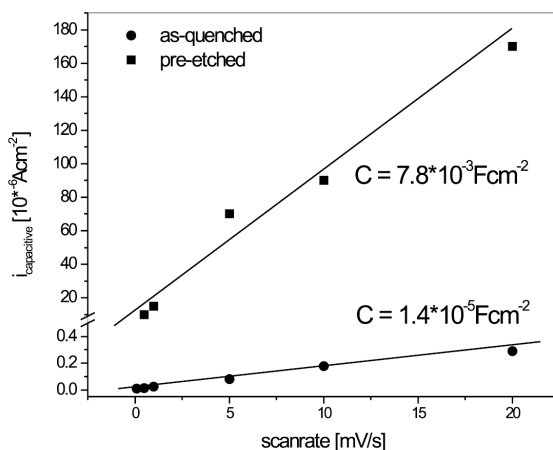
Furthermore, amorphous Zr-Al-Cu-Ni alloys are of special interest regarding their interaction with hydrogen which is mainly related to the combination of early and late transition metals (ETM-LTM). The first step of an electrolytical hydrogen charging process (schematically illustrated in Fig. 1) is the cathodic reduction of protons or water molecules at the metal surface to form adsorbed hydrogen atoms. These atoms can recombine to form molecular hydrogen or they are absorbed into the bulk metal. In amorphous ETM-LTM alloys, absorbed hydrogen occupies tetrahedral interstitial site types (n) at different energy levels (E_n) which exist at a certain probability in the chemically random structure [6]. Theoretically, amorphous alloys have a high number of coordinatively unsaturated surface atoms. Therefore, a high activity for electron transfer reactions is expected. For melt-spun amorphous Zr-based alloys from capacity measurements (Fig. 2) a significant increase of the active surface area after pre-etching in low concentrated hydrofluoric acid, which obviously removes air-formed surface oxides, can be concluded. Compared to the corresponding crystalline alloy the cathodic hydrogen reduction was found to generally take place at lower overpotentials on the amorphous alloy surface. For two glassy Zr-Al-Cu-Ni alloys the electrochemical hydrogenation and the effect of hydrogen on their thermal

Fig. 1 Schematic illustration of the cathodic hydrogen reduction and the hydrogen absorption of an amorphous ETM-LTM alloy



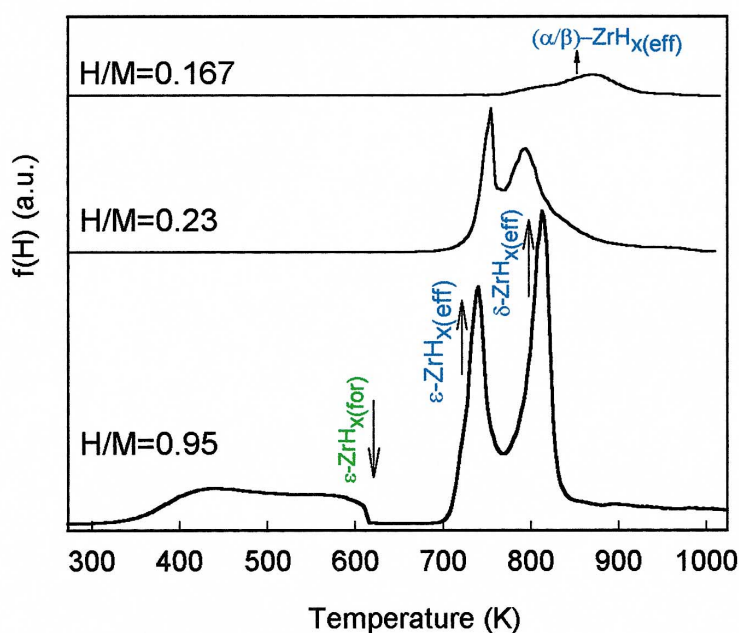
For melt-spun amorphous Zr-based alloys from capacity measurements (Fig. 2) a significant increase of the active surface area after pre-etching in low concentrated hydrofluoric acid, which obviously removes air-formed surface oxides, can be concluded. Compared to the corresponding crystalline alloy the cathodic hydrogen reduction was found to generally take place at lower overpotentials on the amorphous alloy surface. For two glassy Zr-Al-Cu-Ni alloys the electrochemical hydrogenation and the effect of hydrogen on their thermal

Fig. 2 Capacity measurements performed in 0.1 N NaOH on the amorphous $Zr_{59}Ti_3Al_{10}Cu_{20}Ni_8$ alloy surface in the as-quenched state and after pre-etching in 0.01 M HF



behaviour have been studied in detail [7,8]. By short-term charging in strong alkaline electrolyte at room temperature, a maximum hydrogen-to-metal ratio (H/M) of 1.5 for the $Zr_{55}Cu_{30}Al_{10}Ni_5$ and of 1.65 for the $Zr_{65}Cu_{17.5}Al_{7.5}Ni_{10}$ alloy was obtained while keeping the amorphous structure. Differential scanning calorimetric investigations (DSC) on samples with different H/M-ratios indicate a significant decrease in thermal stability, i.e. a reduction of the supercooled liquid region and a complete change in the crystallisation sequence with increasing hydrogen content. Following the effusion of hydrogen by thermal desorption analysis (TDA) (Fig. 3) reveals that the desorption process can be divided in two distinct stages. This is in particular visible for very high hydrogen contents, where the curve shows one rather broad desorption maximum below 623K and a second stage, starting at about 673K which is characterised by the appearance of two sharp desorption peaks. In the first stage hydrogen desorbs from high interstitial-site energy levels. Zirconium hydrides are formed equally above 623K. At higher temperatures partial desorption of hydrogen occurs. Simultaneously, transformation to hydride phases with lower hydrogen contents takes place in the order: tetragonal ϵ -Zr-hydride, cubic δ -Zr-hydride and a mixture of $(\alpha+\beta)$ -Zr-hydrides. Samples with lower hydrogen content do not desorb hydrogen below 623K, indicating that hydrogen is captured in interstitial sites corresponding to low energy levels with high affinity to hydrogen.

X-ray diffraction (XRD) and transmission electron microscopy (TEM) after annealing were used to study the crystallisation process of differently hydrogen-charged samples. For $Zr_{65}Cu_{17.5}Al_{7.5}Ni_{10}$ hydrogen was found to suppress the oxygen-triggered formation of metastable phases, in particular of the quasicrystalline phase [9]. Furthermore, hydrogen supports copper segregation which is detectable after slow electrolytic charging to very high H/M ratios at room temperature as well as after heating amorphous Zr-Al-Cu-Ni samples even with low hydrogen content. Hence, nanocrystalline Cu-rich phases are the primary products formed upon crystallisation, as obvious from the TEM image in Figure 4. At high H/M ratios, a severe

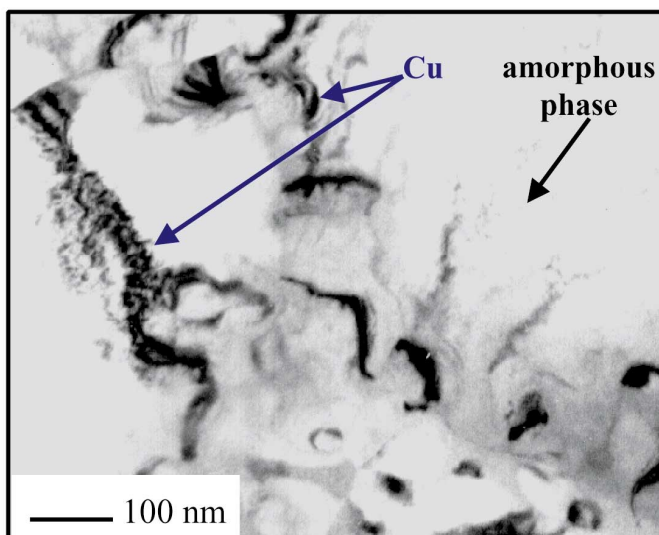


preferential Zr-hydride formation causes enrichment of Cu, Ni and Al in the residual amorphous phase which results in the crystallisation of new stable intermetallic compounds.

In current experiments, the diffusivity of hydrogen in the amorphous alloy compared to that in the crystalline counterpart is studied. Results of these investigations are shown in Fig. 5. In the amorphous alloy, the hydrogen diffusivity upon cathodic charging is four times larger and in contrast to the crystalline alloy, it does not follow the regular Sievert's law [10]. The hydrogen diffusivity in the amorphous alloy increases with increasing hydrogen content, i.e. the diffusion coefficient varies with the hydrogen concentration in the material.

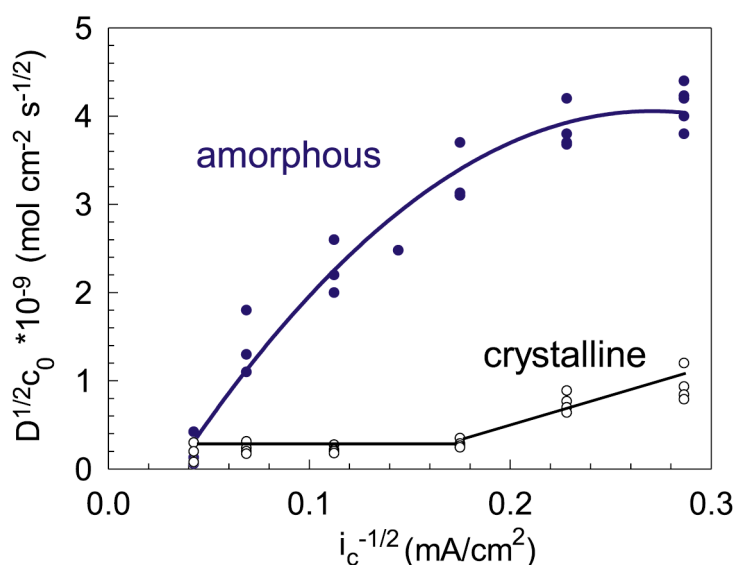
Fig. 3 TDA curves of differently hydrogen-charged amorphous $Zr_{55}Cu_{30}Al_{10}Ni_5$ samples (heating rate: 15 K/min) ((for)... formation; (eff)... effusion)

Fig.4 TEM bright-field image of $Zr_{65}Cu_{17.5}Al_{7.5}Ni_{10}$: hydrogen-charged to H/M=0.4 and subsequently heated to the crystallisation temperature



The difference is explained by the fact, that in crystalline alloys only one type of interstitial sites – tetrahedral or octahedral depending on the lattice type – is occupied by hydrogen, whereas in the amorphous structure tetrahedral sites at different energetic levels are present, which are successively filled with hydrogen. At first, sites at the lowest level are filled which is related to a low diffusivity. With increasing hydrogen uptake hydrogen occupies sites at higher energy levels making its diffusion through the amorphous structure easier.

Fig. 5
Results of diffusivity measurements at different cathodic current densities for the amorphous and the crystalline $Zr_{55}Cu_{30}Al_{10}Ni_5$ alloy



Co-operations

Tohoku Univ. Sendai, Japan;
NRC Cairo, Egypt; Inst. for Physical
Chemistry of the Academy of
Sciences, Warsaw, Poland;
Univ. Dortmund

Funded by

DFG

References

- [1] A. Inoue: Bulk Amorphous Alloys: Preparation and Fundamental Characteristics, in Materials Science Foundations, Vol. 4, eds. M. Magini, F.H. Wöhlbier, Zürich: Trans Tech Publications, 1998
- [2] W. L. Johnson: Mater. Sci. Forum 225–227 (1996) 35
- [3] A. Reger-Leonhard, M. Heilmair, J. Eckert: Scripta mater. 43 (2000) 459
- [4] J. C. Turn, R.M. Latanision: Corrosion 39 (1983) 271
- [5] A. Gebert, K. Buchholz, A. Leonhard, K. Mummert, J. Eckert, L. Schultz: Mater. Sci. Eng. A267 (1999) 294
- [6] J. H. Harris, W.A. Curtin, M. Tenhover: Phys. Rev. B 36 (1997) 5984
- [7] N. Ismail, M. Uhlemann, A. Gebert, J. Eckert: J. Alloys Comp. 298 (2000) 146
- [8] N. Ismail, A. Gebert, M. Uhlemann, J. Eckert, L. Schultz: J. Alloys Comp. 314 (2001) 170
- [9] J. Eckert, N. Mattern, M. Zinkevitch, M. Seidel: Mater. Trans., JIM 39 (1998) 623
- [10] A. Sievert: Z. Phys. Chemie 77 (1911) 591

